

Measurement of a Complete Set of Nuclides, Cross-sections and Kinetic Energies in Spallation of ^{238}U 1A GeV with Protons.

P. Armbruster¹, J. Benlliure^{1,2}, M. Bernas³, A. Boudard⁴, E. Casarejos^{2*},
S. Czajkowski⁵, T. Enqvist^{1†}, S. Leray⁴, P. Napolitani^{1,3}, J. Pereira², F. Rejmund^{1,3},
M.-V. Ricciardi¹, K.-H. Schmidt¹, C. Stéphan³, J. Taieb^{1,3‡}, L. Tassan-Got³, C. Volant⁴.

¹ *Gesellschaft für Schwerionenforschung, Planckstr. 1, 64291 Darmstadt, Germany*

² *Universidad de Santiago de Compostela, 15706 Santiago de Compostela, Spain*

³ *Institut de Physique Nucléaire, BP 1, 91406 Orsay Cedex, France*

⁴ *DAPNIA/SPhN, CEA/Saclay, 91191 Gif sur Yvette Cedex, France and*

⁵ *CEN Bordeaux-Gradignan, Le Haut-Vigneau, 33175 Gradignan Cedex, France*

Spallation residues and fission fragments from 1A GeV ^{238}U projectiles irradiating a liquid hydrogen target were investigated by using the FRagment Separator at GSI for magnetic selection of reaction products including ray-tracing, energy-loss and time-of-flight techniques. The longitudinal-momentum spectra of identified fragments were analysed, and evaporation residues and fission fragments could be separated. For 1385 nuclides, production cross-sections covering 3 orders of magnitude with a mean accuracy of 15%, velocities in the U-rest frame and kinetic energies were determined. In the reaction all elements from uranium to nitrogen were found, each with a large number of isotopes.

PACS numbers: 25.40.Sc, 25.85.Ge, 28.41.Kw, 29.25.Rm

In view of the importance of proton-induced spallation reactions in the 1 GeV range for future technological applications and the unique experimental possibilities at GSI [1, 2], Darmstadt, a program was initiated to measure isotopic cross-sections and kinetic energies. ISOL-separators world-wide use the proton on ^{238}U reaction since 35 years, and future radioactive-beam facilities producing neutron-rich isotopes count on it, but a solid base for the primary isotopic production is missing. By 1 GeV protons two main reaction channels are populated: Spallation Evaporation Residues (EVR) and Fission Fragments (FF). In the 1960's G. Friedlander and collaborators were the first, using radiochemical and surface-ionization techniques, who studied the reactions $p + \text{U}$ and $p + \text{W}$ at various energies [3]. Isotopes close to the target-nuclei and of the alkaline elements rubidium and cesium were identified and measured. In the 1970's systematic measurements on all alkalines were undertaken using on-line mass separators [4, 5]. Later investigations of FF's in 1 GeV proton reactions on heavy elements using different techniques were performed [6, 7, 8]. All results on p-induced fission were evaluated recently [9].

A 1A GeV ^{238}U beam from the GSI accelerator facility produced EVR's and FF's in a liquid H_2 -target, 87 mg/cm² thick. The target was provided by DAPNIA-Saclay and IPN-Orsay [10]. Fully stripped residues produced in inverse kinematics and emitted into a small cone

in forward direction were separated with well controlled efficiencies within 0.3 μs by the high-resolution spectrometer FRS [1] and its ToF and ΔE detectors. The high resolving power of the FRS enabled to scan the longitudinal velocity distributions of all isotopes and to analyse the kinematics of the reactions in the uranium rest frame. For further experimental information, see refs. [2, 11, 12]. Based only on physical properties of the radioactive ions, the method does not depend on chemistry. Primary residues are observed, as all β -decay and nearly all α -decay half-lives are longer than the separation times. Finally, cross-sections for about 1400 isotopes and their kinetic energies were determined.

In Fig. 1 we present in a proton-neutron plot cross-sections using a colour logarithmic scale. In this unique comprehensive "transmutation" of uranium, all elements from uranium to nitrogen, each with a large number of isotopes are observed. In a cross-section range of about 3 orders of magnitude 1385 isotopes are observed, as shown on the figure. The total cross-section of (1.97 ± 0.3) b divides in (1.53 ± 0.2) b for fission [12] and (0.44 ± 0.1) for EVR's [11]. It is of primary interest to understand the large fraction (78 %) observed for nuclear fission. For elements beyond tungsten, $Z > 74$, EVR's dominate over fission fragments [11], whereas FF's identified by their kinematics of a binary break-up process populate all the range below tungsten down to the lightest element nitrogen. Data on fission fragments are published for $Z = 28$ to 63 [12]. The missing lightest and the heaviest elements, $Z = 7-31$ [13] and $Z = 64-74$ [14], respectively, accomplish the full distribution which is presented as a high-light of this letter.

Fig. 2 a) b) show integrated distributions of cross-sections depending on atomic and neutron numbers. The Z-distribution of EVR's, Fig. 2a, decreases steadily going to lighter elements down to $Z = 74$. A shoulder is

*Present address: Centre de Recherches du Cyclotron, UCL, B-1348 Louvain-la-Neuve, Belgium

†Present address: CUPP-project P. O. Box 22 FIN-86801 Pyhäsalmi, Finland

‡Present address: CEA/Saclay DM2S/SERMA/LENR, 91191 Gif/Yvette CEDEX, France

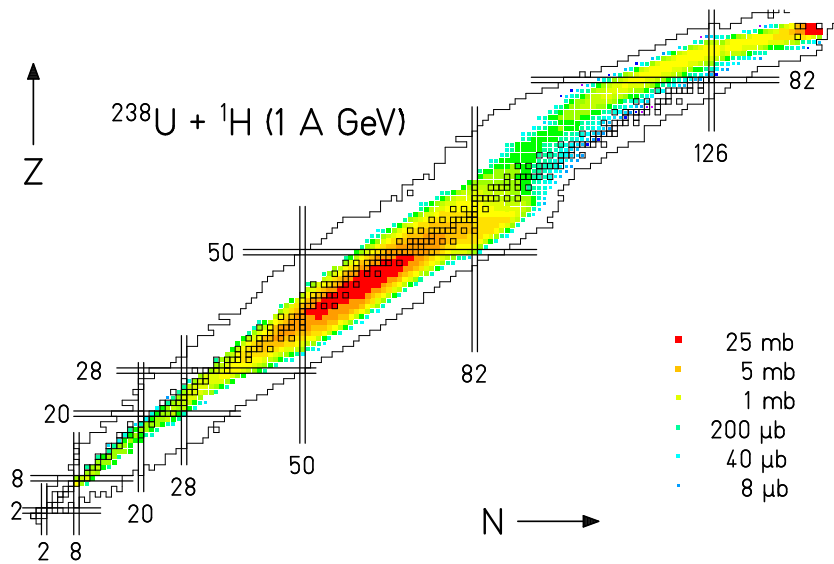


FIG. 1: The identified isotopes are shown on a chart of nuclei. Numerical values are available on <http://www-w2k.gsi.de/kschmidt/data.htm>. The logarithm of the experimental cross-sections are indicated by a color scale.

seen in the range $Z = 80$ to 88 . The distributions of FF's reveal a small 5% contribution of the classical asymmetric low-energy fission [12]. The underlying parent nuclei are relatively cold. They cluster around ^{233}U , but may reach down to $A_0 = 226$ [15]. Having separated this asymmetric contribution from the total Z -distribution, a mean atomic number of $Z = 44.9$ is found. The remaining distribution is surprisingly symmetric and has a standard deviation of 6.4 charge units. A contribution from lighter fissioning parent nuclei, which should increase the cross section of the lighter part of the distribution is barely visible in the range $Z = 20$ to 30 . At very large mass-asymmetries of the FF's, $Z_1/Z_2 < 20/70$, the cross sections pass a minimum and increase slightly for most extreme asymmetries. This was seen before [16] and is explained by the Businaro-Gallone mountain [17] in the liquid-drop potential energy surface (LDM-PES). The N -distribution of EVR's, Fig. 2b, shows an extended plateau between $N = 138$ and $N = 110$ at a low level of (5.0 to 6.4) mb which specifies highly fissile parent nuclei ($Z_0^2/A_0 > 34$). These small cross sections are observed for spherical nuclei around $N = 126$ having large ground-state shell-corrections and thus also increased fission barriers. At the excitation energies of the fissioning parent nuclei produced in our reaction, the higher barriers give no increased survival against fission. The enhanced fission probabilities at $N = 126$ are explained by the low level densities for nuclei with spherical ground states [18]. Small cross-sections are observed as well for highly fissionable nuclei, being deformed and having much smaller ground-state shell-corrections at the upper limit $N = 138$ of the plateau. They are found even down at the lower limit, $N = 110$ in the region of $Z = 80$ to 82 . Finally, in

the range of $N = 110$ to 100 , cross sections break down. At 1A GeV the excitation energy transferred in the reaction approaches its upper limit at about 500 MeV for mass-losses of $\Delta A > 50$. The N -distribution of FF's, Fig. 2b, peaks at $N = 62.4$. The low-energy asymmetric fission subtracted, we obtain the high-energy symmetric distribution with a mean neutron number of 61.9. Combined with the mean proton number 44.9 obtained from the Z -distribution a mean mass number of $A = 106.8$ is reconstructed for FF's of high-energy symmetric fission. A small surplus of cross section at $N = (30 \pm 6)$ may indicate fission from lighter parent nuclei down in the range of $Z_0 = 80 \pm 4$. These could be the asymmetric fragments of the tail of the symmetric fission channel, originating from fissioning parent nuclei located at the lower limit in the plateau and in its fall.

The measured standard deviation of the high-energy symmetric Z -distribution, Fig. 2a, of $\sigma_Z = 6.4$ a.u. is related via the curvature of the LDM-PES to the excitation energy of the mean parent nucleus at the fission barrier [19, 20, 21]. With a fission barrier of 4 MeV, an energy above ground state of (58 ± 10) MeV is obtained, allowing for an emission of 6 neutrons. Adding these neutrons emitted from the fragments to the neutron number of the mean pair of fragments (2×61.9), a neutron number of $N_0 = (130 \pm 1)$ follows for the mean parent nucleus. ^{220}Th is the mean parent nucleus reconstructed from the isotopic distribution of FF's.

For the complete set of FF's produced in the reaction, we obtain for each element the mean neutron to proton ratio \bar{N}/Z and the width of its isotopic distribution $\sigma_N^{Z=const.}$. These values are shown in Fig. 3 a), b) separated into low-energy asymmetric and high-energy sym-

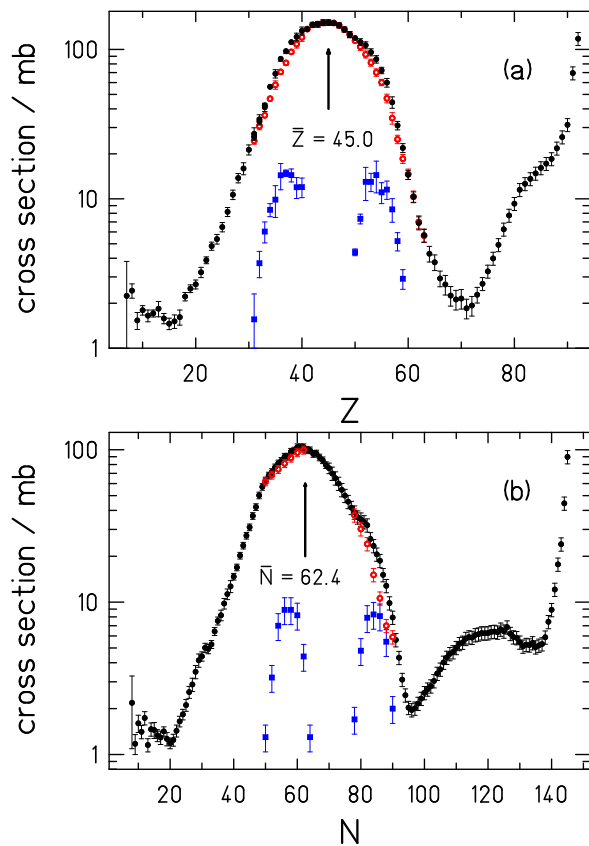


FIG. 2: a) Measured Z -distribution for all elements between $Z = 7$ and 92 ; b) Measured N -distribution for all neutron numbers between $N = 8$ and 146 . The total cross sections (full point), cross section for low-energy asymmetric fission (blue square) and for high-energy fission (red empty point) are reported separately.

metric fission. They describe the isospin dependences of the cross sections. The \bar{N}/Z -ratio of the mean fission fragment ^{107}Rh , 1.38, is found smaller than for low-energy energy fission where $\bar{N}/Z = 1.53$.

Fig. 3a shows in the range $Z = 34$ to 56 increasing \bar{N}/Z -ratios for high-energy symmetric fission. The slope observed agrees with a charge-polarisation expected for a smooth LDM-PES showing no nuclear structure effects[22]. A new finding is the rapid decrease of the mean neutron density for isotopes at higher asymmetries. Taking ^{220}Th as the mean parent nucleus and the most asymmetric pair observed $Z_1/Z_2 = 16/74$, mean neutron numbers $N_1/N_2 = 19/99$ are reached summing up to 118 neutrons present in the FFs. 12 neutrons are lost indicating a high excitation energy of about 100 MeV, which is distributed in the high-energy regime between the pair of FFs proportionally to their masses. The heaviest elements lose up to 10 neutron, and beyond erbium, $Z > 68$, all isotopes observed are stable or proton-rich. Neutron-rich isotopes in the wings of the Z -distribution will come

with very low cross sections for the higher elements. It is the small contribution of low-energy asymmetric fission of $(105 \pm 10)\text{mb}$ which stays the main source of neutron-rich isotopes for elements in the range of $Z = 28-64$ [23].

The standard deviation $\sigma_N^{Z=\text{const}}$ of the isotopic distribution for a given element is presented in Fig. 3b. The mean value of $\sigma_N^{Z=\text{const}} = (3.3 \pm 0.2)$ a.u. compares well to $\sigma_N^{Z=\text{const}} = (3.2 \pm 0.7)$ a.u. measured in ^{238}U 0.75A GeV on ^{208}Pb [24]. For asymmetric low-energy fission, $\sigma_N^{Z=\text{const}} = (1.8 \pm 0.2)$ a.u. agrees with $\sigma_N^{Z=\text{const}} = (1.7 \pm 0.05)$ a.u. from ^{238}U 0.75A GeV on ^{208}Pb [25]. High-energy symmetric fission shows a mean standard deviation wider by a factor 1.8 compared to asymmetric low-energy fission. The ratio of standard deviations for the two fission mechanisms decreases from 2.2 for barium ($Z = 56$) to values close to one for the lighter elements. This trend to a larger width of the isotopic distributions going to heavier elements reflects the widening of the LDM-PES in the $(N-Z)$ -degree of freedom and the extended range of isotopes contributing to fission. As observed for the \bar{N}/Z ratio, $\sigma_N^{Z=\text{const}}$ decreases for $Z > 56$. The shift to

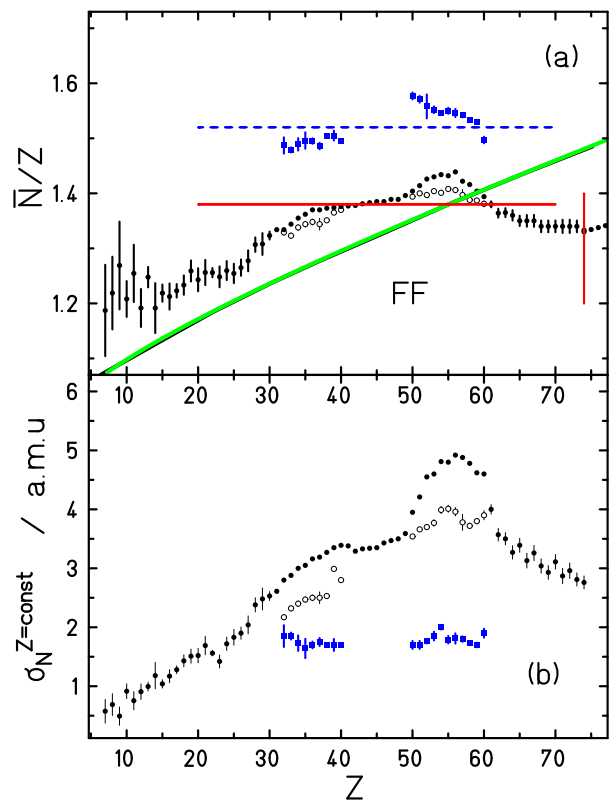


FIG. 3: a) The mean isotopic neutron number \bar{N}/Z and b) the standard deviation $\sigma_N^{Z=\text{const}}$ are plotted as function of the atomic number. Symbols present the different contributions (see Fig. 2). The valley of stability (green line) and the mean N/Z ratio for low-energy asymmetric process (dashed blue-line) and high-energy process (red line) are indicated. The vertical arrow at $Z = 74$ separates fission fragments from spallation residues.

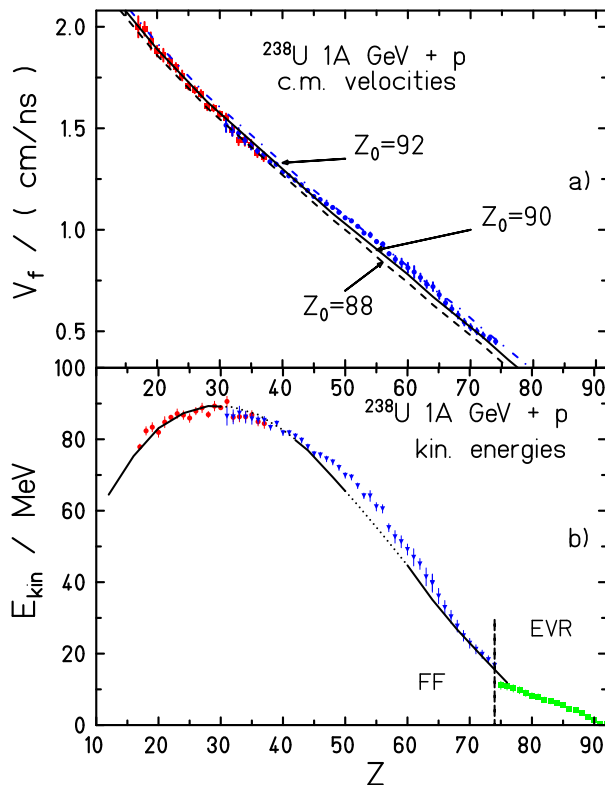


FIG. 4: a) The c.m. velocity of fission fragments measured as a function of the atomic number. The three lines: dashed $Z_0 = 88$, full line $Z_0 = 90$, and dashed-dotted line $Z_0 = 92$, are calculated assuming Coulomb repulsion with a radius constant r_0 being kept constant and fixed by the measured value of the velocity for symmetric fission of ^{220}Th taken as normalisation. The blue triangles and the red points refer to ref. [12] and to ref. [13] respectively. b) The kinetic energies of the isotopes as a function of the atomic numbers, symbols as above and green squares from ref. [11]. The full line is a calculation for ^{220}Th using the conditions as in the legend above. Asymmetric fission contributes in the regions indicated by the dotted lines.

smaller values for elements between $Z = 58-74$ is also visible in Fig. 1 showing the long plane of low cross sections coloured in green.

Fig. 4 a) b) shows the mean velocities of FF's in the U-rest frame and kinetic energies for the elements produced as EVR's or FF's. The mean velocities of FF's, Fig. 4a, show a dependence which demonstrates the small number of elements dominating the family of parent nuclei in the range $Z_0 = (88-92)$. The systematic measurement of kinetic energies of spallation EVR's, Fig. 4b, is a primer achieved by our experimental method. Their kinetic energies are very small, on the average about 2.9 MeV. In this energy range slowing down of heavy ions mainly proceeds by elastic collisions. The maximum of kinetic energies at one third of the atomic number of the parent nucleus, as expected for symmetric fission of a monoisotopic fission source, is experimentally verified.

The complete data-set presented is a main step forward, which in this letter stands for itself. Certainly our work is not finished here. The tasks to be done in the near future are open:

- The energy dependence of the cross sections is hardly known. Further measurements at lower energies are needed for our reaction.
- Our data should serve as a bench mark for simulation codes of the complex physics of spallation reactions with the final goal to predict unknown systems.
- An innovative measuring technique giving more and more precise and complete results generates a better understanding of the underlying physics. Further contributions to fundamental aspects of spallation reactions may still emerge in a coming analysis.

Financial support by EU-contract ERBCHBCT940717 for J. B., T. E. and F. R. and by GSI for P. N., M. V. R. and J. T. is gratefully acknowledged. This work was partially supported by the European Union in the HINDAS project (contract FIKW-CT-20000-00031), and by the support to the access to large facilities (contract EC-HPRI-CT-1999-00001.).

-
- [1] H. Geissel *et al.* Nucl. Instr. Methods **B70** 286 (1992)
 - [2] T. Enqvist *et al.* Nucl. Phys. **A686** 481 (2001)
 - [3] G. Friedlander *et al.* Phys. Rev. **129**, 1809 (1963)
 - [4] R. Klapisch *et al.* Nucl. Instr. Methods **53**, 216 (1967)
 - [5] B. N. Belyaev *et al.* Nucl. Phys. **A348**, 479 (1980)
 - [6] B. A. Bochagov *et al.* Sov. J. Nucl. Phys. **28(2)**, 91 (1978)
 - [7] L. A. Vaishnene *et al.* Z. Phys. **A302**, 143 (1981)
 - [8] Yu. Titarenko *et al.* Nucl. Instr. Meth. **A414**, 73 (1998)
 - [9] A. V. Prokofiev Nucl. Instr. Meth. **463**, 557 (2001)
 - [10] P. Chesny *et al.* GSI-Ann. Rep. 1996, GSI 1997-1, p. 190
 - [11] J. Taieb *et al.* Nucl. Phys. **A724** 413 (2003)
 - [12] M. Bernas *et al.* Nucl. Phys. **A725**, 213 (2003)
 - [13] V. Ricciardi, PhD Thesis, University of Santiago (2004)
 - [14] M. Bernas *et al.* to be published (2004)
 - [15] K.-H. Schmidt *et al.* Nucl. Phys. **A665** 221 (2000)
 - [16] D. G. Sarantites *et al.* Phys. Lett. **B218** 427 (1989)
 - [17] U. Businaro and S. Gallone Nuovo Cimento **1**, 1277 (1955)
 - [18] A. R. Junghans *et al.* Nucl. Phys. **A629**, 635 (1998)
 - [19] A. Ya. Rusanov *et al.* Phys. At. Nucl. **60**, 683 (1997)
 - [20] S.I. Mulgin *et al.* Nucl. Phys. **A640**, 375 (1998)
 - [21] J. Benlliure *et al.* Nucl. Phys. **A700**, 469 (2002)
 - [22] P. Armbruster *et al.* Nucl. Phys. **A140** 385 (1970)
 - [23] M. Bernas *et al.* Phys. Lett. **B415** 111 (1997)
 - [24] W. Schwab *et al.* Eur. Phys. J. **A2**, 179 (1998)
 - [25] C. Donzaud *et al.* Eur. Phys. J. **A1**, 407 (1998)